

Polyelectrolyte Poly(*tert*-butyl acrylate)-*block*-poly(2-vinylpyridine) Micelles in Aqueous Media

Karel Procházka*

Department of Physical and Macromolecular Chemistry, Faculty of Science, Charles University in Prague, Albertov 2030, 128 40 Prague 2, Czech Republic

Thomas J. Martin,[†] Petr Munk,* and Stephen E. Webber*

Department of Chemistry and Biochemistry and Center for Polymer Research, University of Texas at Austin, Austin, Texas

Received April 15, 1996; Revised Manuscript Received July 5, 1996[®]

ABSTRACT: Poly(*tert*-butyl acrylate)-*block*-poly(2-vinylpyridine), PBA-*b*-PVP, was prepared by living anionic polymerization. Polymolecular spherical micelles with compact hydrophobic PBA cores and protonated PVP shells in acid water were prepared by a dialysis from organic–aqueous mixtures and are stable if the pH is less than pH 4.8. The stretching of the PVP blocks in shells depends on pH and ionic strength of the solution and decreases significantly in a narrow pH region below 4.8. Small hydrophobic molecules, such as benzene, may be solubilized into micellar core swelling the core and releasing the segmental mobility of core-forming blocks. Two fluorimetric techniques for determination of pyrene partitioning between micelles and the aqueous phase were used. The first method is based on measurements of the ratio of intensities of the first and third vibrational bands, I_1/I_3 , in the emission spectra of pyrene solubilized in a micellar solution as a function of micellar concentration. The second method is based on the quenching of fluorescence from solubilized pyrene by thallium salts. The two experimental techniques yield close values of the apparent partition coefficient, $K_{app} = 1.3 \times 10^5$ and 1.1×10^5 , respectively.

Introduction

Block copolymers containing strongly hydrophobic and strongly hydrophilic blocks form multimolecular micelles in water and in aqueous buffers in a relatively broad range of pH and ionic strengths, copolymer concentrations, and temperatures.^{1–3} A typical water-soluble copolymer micelle (e.g., polystyrene-*block*-poly(methacrylic acid) micelle) consists of a very dense and compact core formed by several tens to few hundreds hydrophobic insoluble blocks and of a soluble shell formed by partially ionized and fairly stretched polyelectrolyte blocks.² Despite extensive experimental data on micellization of nonpolar block copolymers in organic selective solvents,⁴ only a few micellizing systems of polyelectrolytes in water and aqueous buffers have been studied systematically and in detail.^{2,3}

Micellar cores formed in water by typical hydrophobic polymers that cannot swell in water are very dense and, if the glass-transition temperature of the core-forming blocks is higher than the ambient temperature, the core is in the glassy state. Micellization equilibrium of such copolymers is kinetically frozen and this is the reason why amphiphilic high-molar-mass copolymer chains do not dissolve in aqueous media. Micelles usually have to be prepared by a continuous or stepwise dialysis from miscible organic solvent–water mixtures in which the samples undergo a reversible closed association.^{2a} In this paper we will use the term “micelle” to denote a spherical core/shell structure whether or not they are at thermodynamic equilibrium.

Because only a few systems of amphiphilic micellizing copolymers in water have been studied so far, a reliable general description of the micellization of block poly-

electrolytes in water is still missing. A systematic search for new micellizing systems and studies of their behavior are therefore needed. Micellizing block copolymers containing poly(2-vinylpyridine) blocks have been studied by only a few groups.^{30,p} Poly(2-vinylpyridine) (PVP) is protonated and soluble in aqueous solutions at low pH and is deprotonated and insoluble at a pH higher than 5. The solubility of PVP at low pH offers the possibility to prepare micelles with hydrophobic cores, e.g., polystyrene, or poly(*tert*-butyl acrylate) cores and PVP shells from the corresponding diblock copolymers.

In this paper we study the behavior of micellizing poly(*tert*-butyl acrylate)-*block*-poly(2-vinylpyridine) sample (PBA-*b*-PVP). In the next paper⁵ we describe the complex pH-controlled formation of colloid particles with the three layer onion-type structure from PBA-*b*-PVP and poly(2-vinylpyridine)-*block*-poly(ethylene oxide) copolymer during pH-titration.

Experimental Section

(a) Materials. Purification of Tetrahydrofuran (THF). THF was predried by stirring with CaH₂ overnight. It was then cryodistilled to another flask, where it was treated with and twice distilled from a green sodium/naphthalene complex. This flask was kept under vacuum on the vacuum line until needed for polymerization.

***tert*-Butyl acrylate** was passed through an Al₂O₃ column to remove the inhibitor. Then it was predried over CaH₂ for several hours. It was cryodistilled into another flask, where it was treated with diisobutylaluminum hydride and triethylaluminum⁶ (both 1.0 M in hexane) slightly above –78 °C. It was then cryodistilled again into a modified, pressure equalizing, dropping funnel (an ampoule) where it was stored under carefully dried nitrogen until it was eventually added to the polymerization reactor.

2-Vinylpyridine was passed through an Al₂O₃ column and predried over CaH₂ overnight. Then it was cryodistilled into another flask covered by a sodium mirror. After a slight purple color developed (indicating end of consumption of impurities

* To whom correspondence should be addressed.

[†] Present address: CONDEA Vista Chemical, 12024 Vista Park Drive, Austin, TX 78726-4026.

[®] Abstract published in *Advance ACS Abstracts*, September 1, 1996.

and the first occurrence of carbanions) it was quickly cryo-distilled into an ampule.

1,1-Diphenylethylene (DPE) (Aldrich) was purified by vacuum distillation from *sec*-butyllithium. When *sec*-butyllithium is added to impure DPE, a green color appears first which is due to benzophenone impurity. Upon further addition the red/orange color appears that indicates the presence of the adduct of *sec*-butyllithium and DPE.

(1,1-Diphenyl-3-methylpentyl)lithium was synthesized directly in the addition ampule. *sec*-Butyllithium 1.0 mmol, in a dilute cyclohexane solution was added to an ampule containing 25 mL of THF and 2.0 mmol of purified DPE.

Solvents. Spectral UV grade organic solvents (Aldrich) were used in this study as purchased. Deionized water was used to prepare the aqueous solutions.

Fluorophores. Recrystallized analytical grade fluorophores (Aldrich) were used.

Synthesis and Characterization of Poly(*tert*-butyl acrylate)-*block*-poly(2-vinylpyridine) (PBA-*b*-PVP). The copolymer was synthesized by a living anionic polymerization technique utilizing a vacuum line and an apparatus described previously.^{2d} An amount of LiCl that corresponded to about a twofold excess of the initiator to be added later was introduced first into the polymerization reactor. Then the reactor was flame-treated and the polymerization solvent (THF) was cryodistilled into it. The impurities in the solvent capable of reactions with the initiator were titrated first by the initiator, (1,1-diphenyl-3-methylpentyl)lithium. Then a precalculated quantity of the initiator was introduced and the reactor was cooled to -78°C . 2-Vinylpyridine was added dropwise and was allowed to react for 1 h. The presence of LiCl slowed down the reaction but it prevented the complexation of lithium counterions with the penultimate pyridine moiety. Complexation would increase the reactivity of the growing anion and cause it to attack the ester function of *tert*-butyl acrylate.⁷ An aliquot of the reaction mixture was withdrawn from the reactor and terminated by methanol and then *tert*-butyl acrylate was added dropwise and allowed to react for 45 min. The reaction was terminated by methanol and the copolymer was recovered by precipitation into 40% methanol in water.

The polymers were characterized by gel permeation chromatography (polystyrene calibration). The poly(vinylpyridine) block had molecular weight $M_w = 27\,000$ and $M_w/M_n = 1.07$. The copolymer was rather polydisperse with $M_w = 79\,000$ and $M_w/M_n = 1.27$, evidently from the poly(*tert*-butyl acrylate) block. The monomer composition of the copolymer was obtained by NMR analysis (from the ratio of aromatic and methyl hydrogens). The weight fraction of poly(vinylpyridine) was 0.50.

Preparation and Characterization of Poly(*tert*-butyl acrylate)-*block*-poly(2-vinylpyridine) Micelles. Multimolecular micelles of PBA-*b*-PVP were prepared as follows. The copolymer sample was dissolved in 1,4-dioxane (70 vol %)/methanol mixture, typically with 10 mg/mL of mixed solvent. This mixture is a very good solvent for both blocks and a rapid and complete dissolution of the copolymer occurs. After dissolution, methanol was slowly added with vigorous stirring to 50 vol % content. This mixture is still a fairly good solvent for the sample studied. Then the aqueous 0.1 M HCl solution was very slowly added under a vigorous stirring up to a total water content of 50 vol %. Micelles first appear at the 12 vol % water content in the solvent mixture. The micellar solution was dialyzed against 0.1 M HCl water solution. The concentration of the copolymer in the water (50 vol %)/organic solvent mixture before dialyzing into 0.1 M HCl was 5×10^{-3} g/mL. The volume of the solution increased during the dialysis and the final copolymer concentration was ca. 2.7×10^{-3} g/mL. During the micelle preparation various hydrophobic compounds may be loaded into micellar cores up to a fairly high content. However, we believe that the low molecular weight solvents are fully removed by the extensive dialysis due to their distribution coefficient between the micellar core and huge excess of water.

Solubilization of Benzene into Micelles. Solubilization of benzene was performed as follows: Volume additions of 0.5

μL of benzene were slowly added to 3 mL of a stirred acid micellar solution directly in the cell. The solution was stirred for 5 min and then was left to equilibrate without stirring for another 5 min after each addition. A gas-tight cell was used to prevent benzene evaporation. We have found that the evaporation from the cell closed by an ordinary Teflon stopper is significant. The solution was stirred vigorously before QELS and fluorescence measurement to check for the phase separation. The stirring of a two-phase mixture causes a pronounced turbidity observable for a relatively long time until the two phases fully separate into two layers. Therefore it is relatively simple to obtain an acceptably precise estimate of the maximum amount of benzene which may be solubilized in the aqueous micellar solution.

(b) Experimental Techniques. Static Light Scattering (SLS). The apparent weight-average molar mass, $M_w^{\text{(app)}}$, and radius of gyration, R_G , of micelles in aqueous media were measured by a modified FICA 50 apparatus and evaluated by the Zimm plots as described elsewhere.⁸ The value of the refractive index increment was estimated as the weighted average on the basis of the copolymer composition and literature data for refractive index increments of homopolymers⁹ (for PBA $dn/dc = 0.13$ mL/g and for PVP $dn/dc = 0.27$ mL/g, so that the value for the sample studied is $dn/dc = 0.20$ mL/g). Since the particle molar mass of micelles is very high, concentrations for light scattering measurement ranged from 10^{-6} to 10^{-4} g/mL. Solutions for measurement were clarified by centrifugation since we have found that adsorption of the copolymer sample on filter material is facile (Acrodisc LC13 PVDF, Gelman) and changes in concentration may occur during ultrafiltration. (See also the accompanying paper.⁵)

Quasi-Elastic Light Scattering (QELS). The apparent hydrodynamic radii, R_H , of micelles were measured using a Brookhaven BI 2030 apparatus with a 72-channel correlator. A He-Ne laser operating at 632.8 nm was used as the light source. The temperature was 25°C and the scattering angle was 90° . The characteristic decay rate, $\langle\Gamma\rangle$, was obtained from the first moment of the line-width distribution using the cumulant method. The effective diffusion coefficient, D_e , was calculated as $D_e = \langle\Gamma\rangle/q^2$, where q is the scattering vector. R_H was then evaluated using the Stokes-Einstein relation. The polydispersity (PD) is given by $\mu_2/\langle\Gamma\rangle^2$.¹⁰

Fluorescence Measurements. Steady-state fluorescence spectra were recorded on a SPEX Fluorolog fluorimeter described elsewhere.^{2a} Polarization spectra were measured using a PTI LS-100 luminescence system.

Results and Discussion

Physical Characterization of the Micelles. It has been found by static and quasielastic light scattering measurements that the micellar mass and size of the PBA-*b*-PVP micelles prepared by the above described procedure are fairly reproducible. The apparent molar mass, radius of gyration, and the second virial coefficient (measured by SLS in 0.1 M HCl) are $M_w^{\text{(app)}} = 14.6 \times 10^6$ g/mol, $R_G = 39.8$ nm, and $A_2 = 5.47 \times 10^{-5}$, respectively. A typical Zimm plot of the light scattering data for micelles (prepared at the concentration $c = 2.7 \times 10^{-3}$ g/mL) is shown in Figure 1. The concentration dependence of the LS data, while unusual, is reproducible. We have found that neither the size nor the molar mass of micelles depend on the copolymer concentration used for preparation in the concentration region up to 8×10^{-3} g/mL in the solution before dialysis into the acid water. The apparent hydrodynamic radius and polydispersity (measured by QELS in 0.1 M HCl) are $R_H = 58$ nm and a PD value of ca. 0.06, respectively. This value is based on 12 independent preparations of micellar solutions. Variation of R_H was always less than ± 2 nm.

We have shown in our previous paper that the ratio R_G/R_H is a very sensitive measure of the polydispersity of micellar systems.^{2b} The theoretical value of this ratio

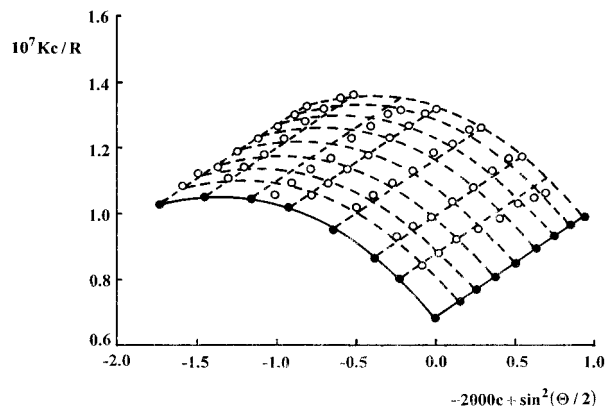


Figure 1. Light scattering Zimm plot for PBA-*b*-PVP micelles in 0.1 M HCl.

for homogeneous spheres is 0.775 and it increases substantially for polydisperse solutes. For our micelles we obtain 0.687, suggesting a low polydispersity. The low value of the experimental ratio is also a consequence of the fact that for inhomogeneous particles the measured gyration radius is only an apparent value. For particles that have a spherical symmetry and are composed of two separate entities, A and B, the apparent radius of gyration, $R_{G,app}$, is given by the following relation

$$R_{G,app}^2 = [R_{G,A}^2 w_A (dn/dc)_A + R_{G,B}^2 w_B (dn/dc)_B] / [w_A (dn/dc)_A + w_B (dn/dc)_B] \quad (1)$$

where $R_{G,i}^2$, w_i , and $(dn/dc)_i$ are the squared radius of gyration, mass fraction, and refractive increment of the i th component, respectively.

For our discussion to follow, the A designation will represent the cores and B the shells. It is reasonable to assume that the cores have a homogeneous segment density. Then $R_{G,A}^2$ is related to the radius of the core, R_C , as

$$R_{G,A}^2 = 3R_C^2/5 \quad (2)$$

We have evaluated R_C from the known micellar mass, composition of the copolymer, and density of PBA assuming no swelling of the core and found $R_C = 14.3$ nm. When evaluating $R_{G,B}^2$ for the shell we must take into account the distribution of the segment density within the shell. If we assume that the segment density is constant throughout the shell, then $R_{G,B}^2$ is given by

$$R_{G,B}^2 = 3R_H^2(1 - A^5)/5(1 - A^3) \quad (3)$$

where $A = R_C/R_H$. Under this assumption we obtain $R_{G,app} = 37.7$ nm and $R_{G,app}/R_H = 0.650$. Assuming that the segment density is inversely proportional to the square of the distance from the micellar center (this corresponds to the model of completely stretched chains in the shell), we find for $R_{G,B}^2$

$$R_{G,B}^2 = R_H^2(1 - A^3)/3(1 - A) \quad (4)$$

For this case $R_{G,app} = 32.1$ nm and $R_{G,app}/R_H = 0.553$. Finally for an intermediate case when the segment density is inversely proportional to the distance from micellar center, $R_{G,B}^2$ is given as

$$R_{G,B}^2 = R_H^2(1 - A^4)/2(1 - A^2) \quad (5)$$

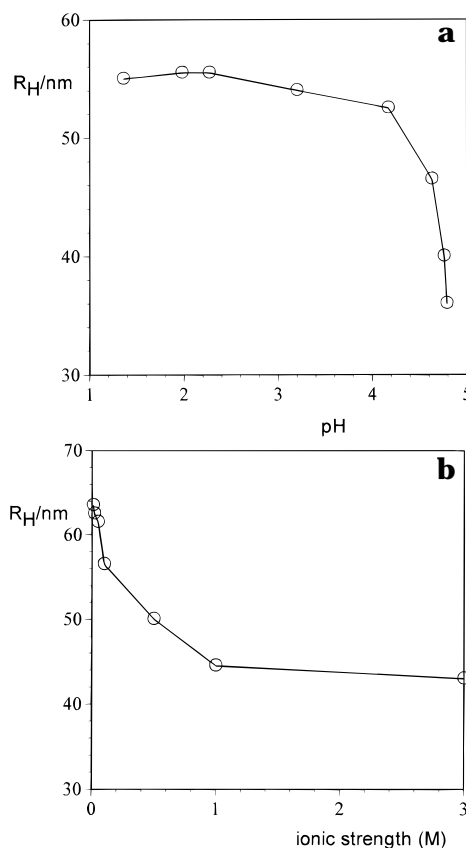


Figure 2. Hydrodynamic radius of PBA-*b*-PVP micelles as a function of (a) pH at ionic strength $I = 0.1$ and (b) ionic strength in HCl/NaCl mixtures at pH 2.3

and $R_{G,app} = 35.3$ nm and $R_{G,app}/R_H = 0.609$. All these values are slightly lower than our experimental value 0.687. This result is compatible with our model of the micelle. More elaborate models of the density profile in spherical brushes have been proposed recently.¹¹ However, polydispersity of micelles (even a very small one, as in our case) complicates the use of complex theoretical models.

Figure 2a shows the hydrodynamic radius, R_H , measured by QELS as a function of pH for the constant ionic strength $I = 0.1$ and Figure 2b shows the decrease in R_H values with increasing ionic strength in aqueous HCl/NaCl mixtures at constant pH 2.3. Both figures suggest significant changes in the shell thickness due to the changing degree of protonation of PVP chains and to the electrostatic screening effect of small counterions.¹¹ The total hydrodynamic radius of PBA-*b*-PVP micelles shrinks from ca. 63 nm at low pH and the lowest ionic strength to 32 nm at the highest pH for which micellar solutions are still thermodynamically stable (pH 4.75 and $I = 0.1$). Thirty-two nanometers is still much larger than the radius of the core ($R_C = 14.3$ nm), which suggests no significant collapse of the shell at this pH. This finding correlates well with the good thermodynamic stability of micelles up to pH values very close to pH 4.8 and indicates that a massive deprotonation of PVP blocks and collapse of micellar shells occurs in a very narrow pH region close to pH 4.8. Micellar solutions with PVP shells can be regarded as pH-buffers and this fact increases their stability in the narrow pH region below pH 4.8. We note that the glassy PBA core can be expected to remain intact for all pH values such that R_h changes reflect the corona only.

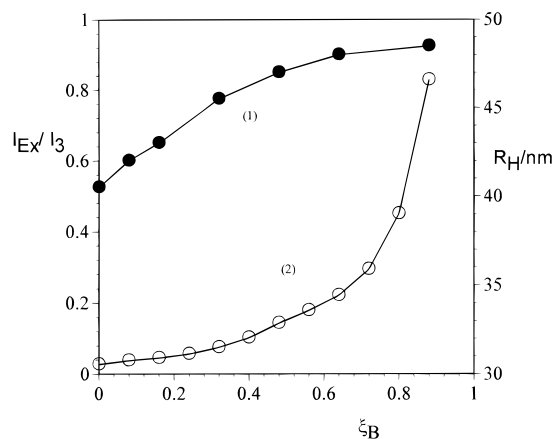


Figure 3. Dependence of the hydrodynamic radius of PBA-*b*-PVP micelles (filled symbols, curve 1) and of excimer to monomer ratio of fluorescent intensities of pyrene solubilized in their cores (open symbols, curve 2) on the amount of benzene in the swollen cores. ξ_B is the mass ratio of benzene to PBA, corrected for the solubility of benzene in water (see text).

Swelling of the Micellar Core by Benzene: Excimer and Depolarization Studies. To probe the rigidity and the properties of the micellar cores, the following experiments were performed: Pyrene was solubilized up to a very high loading into micellar cores during micelle preparation. Typically 0.5 mL of 1 mg/mL pyrene in methanol was added to 5 mL of the 70 vol % dioxane solution used in the earliest step of the micelle preparation (see Experimental Section). The concentration of pyrene was measured by UV absorption in the region of low micellar concentrations and was corrected for the light scattering from micelles. The relative amount of pyrene in micelles was estimated as ca. 400 pyrene molecules per micellar core. For micellar cores with the radius R_C ca. 14.3 nm, this represents a molar concentration of 8.4×10^{-2} mol/L. Despite the small separation (ca. 1.9 nm) between individual pyrene molecules at such a high concentration, no excimer emission was observed. This indicates that the rotational and translational diffusion of the pyrene molecule is almost frozen on the 10^1 – 10^2 ns time scale and the fraction of suitably oriented contact pairs prior to excitation is very low. Similar behavior was observed in our earlier studies^{2b,c} of micellization of polystyrene-*block*-poly(methacrylic acid) copolymers with naphthalene-tagged core-forming blocks. In those studies, a short oligomeric poly(2-vinylnaphthalene) block was attached at the beginning or the end of the PS block and excimer fluorescence, which was very strong in good solvents, disappeared in micellar systems in aqueous solution.

Swelling of the core by small molecules, such as benzene, permits movement of the pyrene molecules and diffusion-controlled excimer fluorescence. Figure 3 shows the effect of the core swelling on the total size of micelles and on the fluorescence properties of solubilized pyrene in micellar solutions in 0.1 M HCl. There is a steady increase of R_H with increasing mass ratio of solubilized benzene-to-PBA block of the copolymer, ξ_B . Values of ξ_B are corrected for the benzene solubility in 0.1 M HCl. This value (1.6 g/L) was estimated by the same procedure used to determine the solubilization limit for micelles. The literature value of benzene solubility in pure water (1.732 g/L) is in good agreement with our estimate. For the evaluation of ξ_B , the partition coefficient of benzene between micelles and the aqueous phase is needed. We have estimated it from

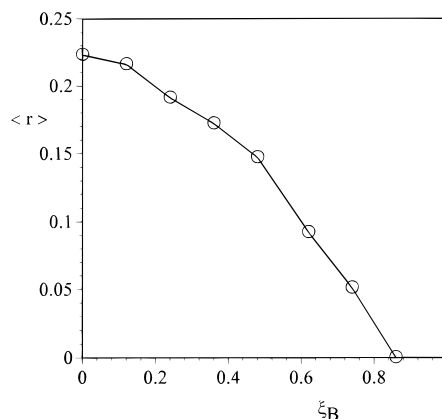


Figure 4. Fluorescence anisotropy of perylene solubilized in the cores of PBA-*b*-PVP micelles as a function of the amount of benzene in the swollen cores.

the difference in the amount of benzene needed to reach saturation in the solvent and in the micellar solution of known concentration. Then we evaluated ξ_B from the known addition of benzene assuming the standard partitioning equilibrium. Values of R_H increase only slightly with increasing content of the swelling agent, since the size of the core represents only a small part of the R_H values. The excimer-to-monomer fluorescence intensity increases sharply above $\xi_B = 0.7$ (monomer emission was measured at 383 nm, the vibrational band I_3 ; excimer emission was measured at 430 nm). It is evident that a relatively large quantity of benzene (comparable with the mass of PBA) is needed to liberate the motion of pyrene molecules in the cores and to enable the formation of excimers.

In another experiment, a relatively small amount of perylene was solubilized into micelles during their preparation. The perylene concentration was then further lowered by dialyzing the solution against 0.1M HCl. The resulting micellar solution contained ca. 5 perylene molecules per micelle and was used for the steady-state fluorescence anisotropy measurements. A very low perylene loading of micelles is needed, since the Förster radius of the perylene–peryrene energy transfer is very large,¹² R_0 ca. 3.5 nm, because of the large overlap in absorption and emission spectra. An efficient nonradiative excitation energy migration at higher perylene loading would partially depolarize the emission and interfere with depolarization mobility studies. The intensity of perylene fluorescence from micelles is high and the precision of the anisotropy measurements is satisfactory. Perylene fluorescence anisotropy, $\langle r \rangle = (I_{||} - I_{\perp}) / (I_{||} + 2I_{\perp})$, was measured as a function of the amount of the solubilized benzene, ξ_B . Perylene was excited at 436 nm using a vertically polarized beam and the parallel and perpendicular fluorescence intensities, $I_{||}$ and I_{\perp} , respectively, were measured at 468 nm. The plot of $\langle r \rangle$ vs ξ_B is shown in Figure 4. The fluorescence anisotropy is quite high in cores without benzene, $\langle r \rangle = 0.22$, and decreases steadily with increasing amount of solubilized benzene. This behavior correlates well with the pyrene excimer-to-monomer fluorescence intensity increase in Figure 3 and demonstrates that complete rotation and diffusion occurs within the ca. 6–7 ns lifetime of the perylene excited state¹³ only when ξ_B reaches a value of about 0.8. Note that under these conditions all perylene remains segregated in the micelle core, as indicated by a complete absence of Tl^+ quenching (data not shown).

Both experiments with pyrene and perylene indicate that the nonswollen cores are compact and the relatively immobile PBA blocks hinder translational and rotational motion of solubilized fluorophores on the time scale of excited state lifetimes, i.e., 10^1 – 10^2 ns.

Partition Coefficient of Pyrene between Micelles and the Aqueous Phase. In the second part of this paper we report our study of the distribution of fluorophores between micelles and the aqueous phase. It is convenient to introduce an apparent partition coefficient, K_{app} , describing the partitioning of pyrene between micelles and the aqueous phase,

$$K_{app} = K_C + bK_S(q_S/q_C) \quad (6)$$

where K_C and K_S are the true partition coefficients of pyrene between cores and the aqueous phase and between shells and the aqueous phase, respectively, b is the ratio of volumes of the shell and the core, and (q_S/q_C) is the ratio of the pyrene fluorescence quantum yields in the shell and the core. As shown in the Appendix, this coefficient may be evaluated either from the measurement of the ratio of the first and third vibrational bands, I_1/I_3 , in the pyrene emission as a function of the micellar concentration or from fluorescence quenching experiments. The pyrene emission I_1/I_3 ratio is environment-sensitive and is often used to probe the pyrene microenvironment polarity.¹⁴ It was successfully used for studying associative processes in polymer solutions and for determination of the distribution of pyrene derivatives in bulk block copolymers.¹⁵ Evaluation of K_{app} based on the quenching experiments is general and it may be used for fluorophores without environment-sensitive vibrational structure.

We have measured the I_1/I_3 ratio in PBA ($I_1/I_3 = 1.07$), PVP (1.46), and PBA-*b*-PVP (1.09) films. The films for measurement were prepared by evaporating solvent from 2 wt % solution in 1,4-dioxane deposited on a quartz disk and by drying in vacuum. The weight ratio of pyrene-to-polymer was 0.03. The value obtained for PVP (1.47) is in a good agreement with the value obtained by Winnik *et al.*¹⁵ The I_1/I_3 value in the PBA-*b*-PVP copolymer film is very close to that in PBA film and suggests that pyrene is in this system confined to the PBA domains. We note that Acree *et al.* have argued that using just the ratio of peaks to assign partitioning can be erroneous because of solvent-dependent quantum yields.¹⁶ Measurement of the I_1/I_3 ratio must be performed very carefully with an apparatus having a high spectral resolution and a constant excitation intensity. All experiments have to be done under the same conditions of spectral resolution. Thus, values obtained using different fluorimeters may significantly differ from each other. Using our fluorimeter, we have measured the uncorrected I_1/I_3 ratio in acid, neutral, and basic water saturated by pyrene; the experimental values were $I_1/I_3 = 1.63$, 1.75, and 1.73, respectively. These values should be corrected for the detector spectral sensitivity (Q_{273}/Q_{282} ca. 0.9) to get the true values which are higher ($I_1/I_3 = 1.90$ in water¹⁴). This apparatus correction factor cancels in the evaluation procedure we use and does not have to be taken into account.

Figure 5 shows the I_1/I_3 ratio for highly pyrene-loaded micelles (ca. 250 pyrene molecules *per* micelle) as a function of polymer concentration. When the total pyrene concentration is significantly higher than its water solubility, the measured values are low and almost constant, $I_1/I_3 = 1.18$, and it is almost impossible

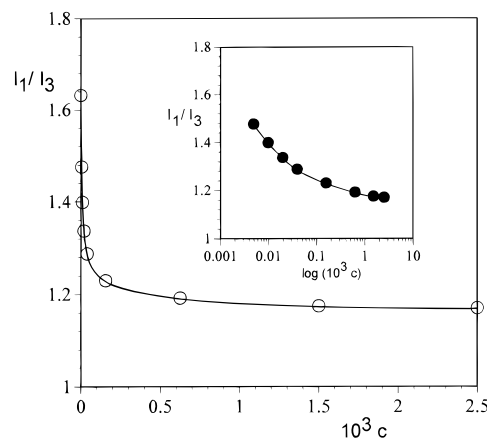


Figure 5. I_1/I_3 ratio of pyrene fluorescence in solutions of PBA-*b*-PVP micelles as a function of polymer concentration; insert, expansion of the low concentration region on a log scale.

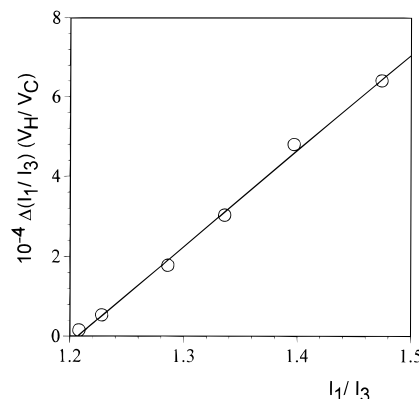


Figure 6. Correlation of the I_1/I_3 data for the evaluation of K_{app} (see text for details). The value of $(V_H/V_C)[(I_1/I_3)_H - (I_1/I_3)]$ is plotted on the y axis.

to quench the fluorescence by Tl^+ (see later discussion). For low concentrations, the measured values rise quite steeply with dilution. Both observations are understandable as the consequence of the equilibrium distribution of pyrene between micelles and the aqueous phase at different micellar concentrations. We have found that the re-equilibration of pyrene in the system after dilution is fairly fast and it is completed on the timescale of tens of minutes. These observations indicate that pyrene diffusion out of these micelles is much faster than in the case of micelles with polystyrene (PS) cores that we have studied earlier.¹⁷ Studies of the release kinetics leading to the evaluation of diffusion coefficients of various fluorophores in micellar PS, PBA, and PVP cores are in progress.

As shown in the Appendix, the linearized plot of $(V_H/V_C)[(I_1/I_3)_H - (I_1/I_3)]$ vs I_1/I_3 is useful for evaluation of the apparent partition coefficient, K_{app} . Values plotted on the y-axis are very sensitive even to small experimental errors and a good linear plot is a severe test of the quality of the data. The plot shown in Figure 6 suggests that the correlation is fairly good. For evaluation of the apparent partition coefficient, K_{app} , the relative quantum yield of pyrene fluorescence in water to that in micellar cores has to be known. We have estimated this quantity from independent measurements. We have measured the fluorescence intensity for a relatively concentrated solution of micelles (ca. $(2-8) \times 10^{-4}$ g/mL) with a fairly high pyrene loading. The concentration of pyrene was estimated using UV absorption. Saturated pyrene solutions in acid, neutral,

and basic water were measured under the same experimental conditions. For concentrated micellar solutions, only a negligible fraction of the fluorescence emission comes from the pyrene molecules located outside the core, since pyrene is accumulated mostly in the cores. The solubility of pyrene at 25 °C was evaluated in acid (0.1 M HCl), neutral, and basic water (0.1 M NaOH) using the published value of the extinction coefficient, $\epsilon_{334} = 5.4 \times 10^4 \text{ L/(mol}\cdot\text{cm)}$ ¹³ to be $3.3 \times 10^{-7} \text{ mol/L}$ in pure water, $3.5 \times 10^{-7} \text{ mol/L}$ in basic water, and $2.5 \times 10^{-7} \text{ mol/L}$ in acid water. The values obtained in this study agree well with the literature solubility data on pyrene in pure water ($3.8 \times 10^{-7} \text{ mol/L}$).¹⁸

In our study, we have been using solutions containing the equilibrium concentration of dissolved oxygen for the following reasons: (a) Repeated freeze–pump–thaw cycles that guarantee quantitative suppression of oxygen-quenching runs the risk of inducing micelle aggregation, although these micelles appear to be quite rugged (for example, they can be redistributed in water after being freeze-dried). Bubbling with Ar does not remove all oxygen and the quantum yields by this method are rather irreproducible. (b) Evaluation of K_{app} does not require the removal of oxygen since we only need to know the relative quantum yield of pyrene fluorescence, $q_{\text{H}}/q_{\text{C}}$, under the conditions of the I_1/I_3 measurements or quenching experiments only. (c) Our experiments allow for a straightforward comparison with the kinetic dilution-quenching experiments that are in progress, which also require knowledge of the $q_{\text{H}}/q_{\text{C}}$ value. We have estimated the ratio $q_{\text{H}}/q_{\text{C}} = 0.55$ under given conditions. Measurements of the I_1/I_3 ratio give the apparent partition coefficient $K_{\text{app}} = 1.3 \times 10^5$. This is very similar to the value of 4×10^5 for phenanthrene^{1a} or 2.2×10^5 for pyrene and 1.1×10^5 for 9,10 diphenylanthracene^{2a} reported earlier for micelles composed of polystyrene-*block*-poly(methacrylic acid) diblocks.

Measurements of pyrene fluorescence in a water–methanol mixture in the presence of protonated PVP indicate that fluorescence is strongly quenched by protonated PVP such that we can assume that q_{S} is small. The second term in the definition of K_{app} (eq 6) is therefore small and we can assume that values of K_{app} and K_{C} are quite close to each other. The large value of this coefficient indicates that at high micellar concentrations most pyrene is solubilized in the micellar cores and its fluorescence cannot be efficiently quenched by water-soluble quenchers, such as Ti^+ , as was observed experimentally.

Pyrene fluorescence from highly concentrated micellar solutions may be quenched easily by solubilizing non-polar quenchers (e.g., CCl_4) into micellar cores. Figure 7 shows the Stern–Volmer plot for the ratio of intensities, I_3^0/I_3 , without and with quencher, respectively, vs weight fraction, ξ_{C} , of the solubilized CCl_4 (concentration of micelles $2.5 \times 10^{-3} \text{ g/mL}$). The linearity of the plot indicates complete accessibility of the quencher to all pyrene molecules. Fluorescence spectra are reproducible and the ratio of I_1 and I_3 intensities does not change with ξ_{C} if measurements are performed rapidly (less than 1 min per spectra) and the system is kept in dark between measurements for at least 30 min. Longer exposure times result in changes of the fluorescence spectra due to photoreactions of pyrene.

In highly diluted micellar solutions, a significant fraction of pyrene resides in the aqueous phase and its emission may be quenched by Ti^+ . Figure 8 shows a typical Stern–Volmer plot, I_3^0/I_3 , for the Ti^+ quenching

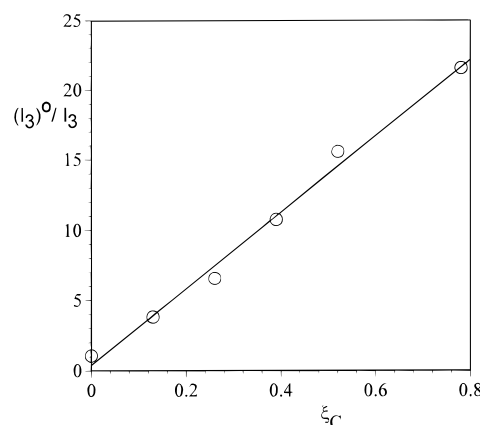


Figure 7. Stern–Volmer plot for quenching by CCl_4 the fluorescence of pyrene solubilized in the cores of PBA-*b*-PVP micelles (ξ_{C} is defined similarly to ξ_{B} in previous plots).

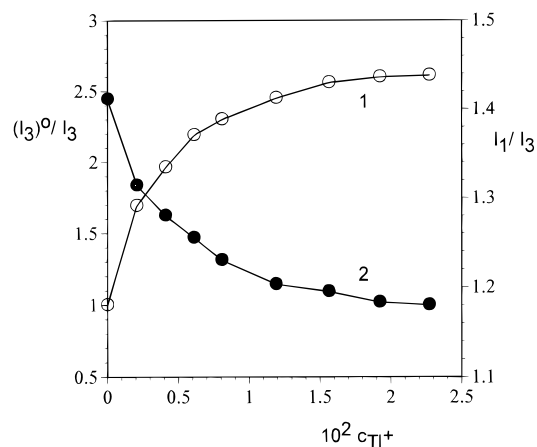


Figure 8. Quenching of pyrene in a solution of PBA-*b*-PVP micelles ($c = 6.4 \times 10^{-6} \text{ g/mL}$) by Ti^+ . The Stern–Volmer plot (curve 1); the dependence of I_1/I_3 on the molar concentration of Ti^+ (curve 2).

(curve 1) and I_1/I_3 (curve 2) for the micellar concentration $c = 6.4 \times 10^{-6} \text{ g/mL}$. The very pronounced downward curvature in the Stern–Volmer plot and the leveling off of I_3^0/I_3 at high quencher concentrations provide a measure of the fraction of fluorophores in cores that are inaccessible to the ionic quencher. When the fluorescence from the water-dispersed fluorophores is completely quenched, the measured I_1/I_3 ratio equals 1.19, which roughly corresponds to the effective $(I_1/I_3)_{\text{M}}$ ratio for micelles. The quenching experiments yield the apparent partition coefficient, $K_{\text{app}} = 1.1 \times 10^5$ for partitioning of pyrene between micelles and the aqueous phase. This value is in good agreement with the value based on the ratio of intensities of vibrational bands, I_1/I_3 (1.3×10^5).

Summary

1. A living anionic polymerization procedure was developed for the synthesis of a block copolymer of *tert*-butyl acrylate and 2-vinylpyridine.

2. Spherical polyelectrolyte PBA-*b*-PVP micelles with compact PBA cores and protonated PVP blocks were prepared in aqueous solution in the pH region below 4.8 and characterized by light scattering techniques. A copolymer sample was dissolved in an organic solvent mixture and the solution was titrated by acid water until polyelectrolyte micelles formed, then the resulting solution was dialyzed into acid water. This procedure yields micelles with a reproducible molar mass and size.

3. The stretching of protonated PVP blocks that make up micellar shells was studied by QELS as a function of pH and ionic strength of the solution.

4. The swelling of micellar cores by solubilizing benzene into micelles was studied using fluorimetric techniques (excimer-to-monomer fluorescence intensity and fluorescence anisotropy measurement for entrapped fluorophores).

5. Fluorimetric techniques (measurements of intensities of the first and third vibrational bands in pyrene emission and the thallium quenching experiments) were applied to estimate the apparent partition coefficient, $K_{app} = (1.1-1.3) \times 10^5$ of pyrene between micelles and the aqueous phase.

Acknowledgment. K.P. acknowledges financial support of this study by the Grant Agency of the Czech Republic (Grant 203/94/0785) and by the Grant Agency of the Charles University (the Charles University Grant 0144/1993). S.E.W. and P.M. acknowledge support by the US Army Grant DAAH04-95-0127. S.E.W. would also like to acknowledge the financial support of the Robert A. Welch Foundation (Grant F-356).

Appendix

1. Evaluation of the Apparent Partition Coefficient, K_{app} , from Quenching Experiments. (a) **General Case.** Fluorescence intensity in a micellar solution with a solubilized fluorophore is a sum of contributions from fluorophore molecules in cores, I_C , in shells, I_S , and in the aqueous phase, I_H . In the linear region of low fluorophore concentrations each contribution, I_i , may be expressed as a product, $I_i = kV_i c_i q_i$, where V_i is the volume fraction of the phase i , c_i is the fluorophore concentration, q_i is the corresponding quantum yield, and k is the apparatus constant. At equilibrium, individual concentrations are not independent but are determined by the total fluorophore concentration, c , and by the partition coefficients between the core and aqueous phase, $K_C = c_C/c_H$, and the shell and aqueous phase, $K_S = c_S/c_H$. Mass balance in the system may be expressed by the following equation

$$c = c_H[V_C(K_C + bK_S) + V_H] \quad (A1)$$

where b is the ratio of volumes of the core and the shell, $b = V_S/V_C$. The total fluorescence intensity, I , may be expressed as follows

$$I = k c_H[V_C(K_C q_C + bK_S q_S) + V_H q_H] \quad (A2)$$

Combination of eqs A1 and A2 gives

$$I = k c q_C \frac{\left(\frac{V_C}{V_H}\right) \left[K_C + bK_S \left(\frac{q_S}{q_C} \right) \right] + \left(\frac{q_H}{q_C} \right)}{\left(\frac{V_C}{V_H}\right) (K_C + bK_S) + 1} \quad (A3)$$

Due to the presence of the instrumental constant in eq A3, it is impossible to obtain any information on partition coefficients from a single measurement of the fluorescence intensity. However, it is possible to obtain it from ratios of intensities measured at different conditions.

Quenching experiments are appropriate for this purpose because they allow for determination of an apparent partition coefficient ($K_{app} = K_C + bK_S(q_S/q_C)$) between micelles and the aqueous phase. By using a

strongly hydrophilic quencher, such as Tl^+ , it is possible to quench the fluorescence in the aqueous phase and possibly also in the shell, without affecting the fluorescence quantum yield in the cores. The quantum yields in the aqueous phase (q_H) and in the shell (q_S) are then lower in the presence of the quencher than those in its absence, i.e., $q_H' < q_H$ and $q_S' < q_S$, while the quantum yield in the core is constant, $q_C' = q_C$. The ratio of fluorescence intensities without and with the quencher, I/I_Q , is given by the following equation

$$\frac{I}{I_Q} = \frac{\left(\frac{V_C}{V_H}\right) \left[K_C + bK_S \left(\frac{q_S}{q_C} \right) \right] + \left(\frac{q_H}{q_C} \right)}{\left(\frac{V_C}{V_H}\right) \left[K_C + bK_S \left(\frac{q_S'}{q_C} \right) \right] + \left(\frac{q_H'}{q_C} \right)} \quad (A4)$$

(b) Special Case. Hydrophobic Fluorophore in Micelles with Positively Charged Shells—Quenching by Positively Charged Ions. In this section we discuss the case of pyrene as a fluorophore and $TlNO_3$ as a quencher. Pyrene fluorescence is strongly quenched by Tl^+ . If a relatively high concentration of $TlNO_3$ (ca. 5×10^{-2} M) is used, emission from pyrene dissolved in water is quenched almost quantitatively and we can assume, in the first approximation, that $q_H' \approx 0$. The shell of PBA-*b*-PVP micelles is formed by protonated and positively charged blocks. A strong electrostatic repulsion hinders the penetration of Tl^+ ions into this positively charged shell. Quenching of the fluorescence from the shell-solubilized fluorophores is in this case very inefficient, and it is reasonable to assume that $q_S' \approx q_S$.

Equation A4 is considerably simplified under the aforementioned assumptions, and it reads

$$\frac{I}{I_Q} = 1 + \left(\frac{q_H V_H}{q_C V_C} \right) \frac{1}{\left[K_C + bK_S \left(\frac{q_S}{q_C} \right) \right]} \quad (A5)$$

The sum in the square brackets of the denominator of the second term of the right-hand side of eq A5 is the apparent pyrene partition coefficient between micelles and water, K_{app} . It may be evaluated from quenching experiments (in the case of pyrene quenching, we use the intensity of the third vibrational band) as

$$K_{app} = \left(\frac{q_H V_H}{q_C V_C} \right) \frac{1}{(I_3/I_{3,Q} - 1)} \quad (A6)$$

In quenching experiments, all quantities in eq A6 are known, except the relative water-to-core pyrene emission quantum yield, (q_H/q_C) . This relative quantum yield may be evaluated from independent measurements.

2. Evaluation of K_{app} from Measurement of the Ratio of I_1/I_3 as a Function of Micellar Concentration. The effective partition coefficient, K_{app} , may be also obtained from measurement of the ratio of intensities of the first and third vibrational bands, I_1/I_3 , as a function of micellar concentration. The first vibrational band is symmetry forbidden and its intensity depends on interactions with the microenvironment. The (I_1/I_3) ratio is often used to probe interactions of pyrene with surrounding molecules.^{14,16}

The intensity I_3 in the micellar solution is given by eq A2. The quantum yield of the first vibrational band, $q_{i,1}$, in microenvironment i (i.e., in the phase, i) may be

expressed by using $q_i \equiv q_{i,3}$ and the corresponding experimental value of $(I_1/I_3)_i$ to yield $q_{i,1} = (I_1/I_3)_i q_i$. Therefore for the experimentally observed ratio, I_1/I_3 , we can write the following relation

$$\frac{I_1}{I_3} = \left[\left(\frac{V_C}{V_H} \right) K_C [(I_1/I_3)_C + b(K_S/K_C)(I_1/I_3)_S(q_S/q_C)] + (I_1/I_3)_H(q_H/q_C) \right] / \left[\left(\frac{V_C}{V_H} \right) [K_C + bK_S(q_S/q_C)] + (q_H/q_C) \right] \quad (A7)$$

In the region of high micellar concentration, the (I_1/I_3) ratio is virtually constant and it is equal to the effective equilibrium $(I_1/I_3)_M$ ratio in micelles

$$(I_1/I_3)_M = [(I_1/I_3)_C + b(K_S/K_C)(I_1/I_3)_S(q_S/q_C)] / [1 + b(K_S/K_C)(q_S/q_C)] \quad (A8)$$

Combination of eqs A7 and A8 with the definition of the apparent partition coefficient, K_{app} , yields a simple equation for the evaluation of K_{app} ,

$$K_{app} = (q_H V_H / q_C V_C) [(I_1/I_3)_H - (I_1/I_3)] / [(I_1/I_3) - (I_1/I_3)_M] \quad (A9)$$

From the experimental point of view, eq A9 is easy to handle. The value of $(I_1/I_3)_M$ may be estimated quite precisely either from the limiting behavior of I_1/I_3 for high micellar concentrations or from a linearized form of eq A9

$$y = (V_H/V_C) [(I_1/I_3)_H - (I_1/I_3)] = [(I_1/I_3) - (I_1/I_3)_M] (q_C/q_H) K_{app} \quad (A10)$$

If values of $[(I_1/I_3)_H - (I_1/I_3)](V_H/V_C)$ are plotted vs (I_1/I_3) , the value $y = 0$ is attained for $(I_1/I_3) = (I_1/I_3)_M$ and the value of K_{app} may be obtained from the slope. The linear plot of experimental points indicates that the system studied behaves according to the model and the scatter in the experimental points allows for testing the quality of the data. A similar approach based on (I_1/I_3) measurements was used by Winnik *et al.*¹⁵ in the study of the behavior of the micellizing system of polystyrene-block-poly(ethylene oxide) in aqueous media. These authors did not take into account solubilization of pyrene into the micellar shell but the formal structure of their equation is similar to eq A9.

References and Notes

- (1) See, for example: Linse, P. *Macromolecules* **1994**, *27*, 6404 and references therein.
- (2) (a) Cao, T.; Munk, P.; Ramireddy, C.; Tuzar, Z.; Webber, S. E. *Macromolecules* **1991**, *24*, 6300. (b) Procházka, K.; Kiserow, D.; Ramireddy, C.; Tuzar, Z.; Munk, P.; Webber, S. E. *Macromolecules* **1992**, *25*, 454. (c) Kiserow, D.; Procházka, K.; Ramireddy, C.; Tuzar, Z.; Munk, P.; Webber, S. E. *Macromolecules* **1992**, *25*, 461. (d) Ramireddy, C.; Tuzar, Z.; Procházka, K.; Webber, S. E.; Munk, P. *Macromolecules* **1992**, *25*, 2541. (e) Tian, M.; Qin, A.; Ramireddy, C.; Webber, S. E.; Munk, P.; Tuzar, Z.; Procházka, K. *Langmuir* **1993**, *9*, 1741.
- (f) Kiserow, D.; Chan, J.; Ramireddy, C.; Munk, P.; Webber, S. E. *Macromolecules* **1992**, *25*, 5338. (g) Chan, J.; Fox, S.; Kiserow, D.; Ramireddy, C.; Munk, P.; Webber, S. E. *Macromolecules* **1993**, *26*, 7016. (h) Qin, A.; Tian, M.; Ramireddy, C.; Webber, S. E.; Munk, P.; Tuzar, Z. *Macromolecules* **1994**, *27*, 120.
- (3) (a) Selb, J.; Gallot, Y. In *Development in Block Copolymers*; Goodman, I., Ed.; Elsevier Applied Science; London, U.K., 1982; Vol. 2, p 27. (b) Gao, Z.; Varshney, S. K.; Wong, S.; Eisenberg, A. *Macromolecules* **1994**, *27*, 7923. (c) Zhang, L.; Eisenberg, A. *Science* **1995**, *268*, 1728. (d) Astafieva, I.; Zhong, X.-F.; Eisenberg, A. *Macromolecules* **1993**, *26*, 7339. (e) Zhang, L.; Barlow, R. J.; Eisenberg, A. *Macromolecules* **1995**, *28*, 6055. (f) Morishima, Y.; Itoh, Y.; Hashimoto, T.; Nozakura, S.-I. *J. Polym. Sci., Polym. Chem. Ed.* **1982**, *20*, 2007. (g) Dan, N.; Tirrell, M. *Macromolecules* **1993**, *26*, 4310. (h) Antonietti, M.; Heinz, S.; Schmidt, M.; Rosenauer, C. *Macromolecules* **1994**, *27*, 3267. (i) Kwon, G. S.; Naito, M.; Yokoyama, M.; Okano, T.; Sakurai, Y.; Kataoka, K. *Pharm. Res.* **1995**, *12*, 92. (j) Kwon, G. S.; Yokoyama, M.; Okano, T.; Sakurai, Y.; Kataoka, K. *Pharm. Res.* **1993**, *10*, 970. (k) Kataoka, K.; Kwon, G. S.; Yokoyama, M.; Okano, T.; Sakurai, Y. *Journal of Controlled Release* **1993**, *24*, 119. (l) Kwon, G. S.; Kataoka, K. *Advanced Drug Delivery Reviews* **1995**, *16*, 295. (m) Harada, A.; Kataoka, K. *Macromolecules* **1995**, *28*, 5294. (n) Scholz, C.; Iijima, M.; Nagasaki, Y.; Kataoka, K. *Macromolecules* **1995**, *28*, 7295. (o) Selb, J.; Gallot, Z. *Makromol. Chem.* **1980**, *181*, 809; 2605. (p) Selb, J.; Gallot, Z. *Makromol. Chem.* **1981**, *182*, 1491; 1513; 1775.
- (4) (a) Tuzar, Z.; Kratochvíl, P. In *Surface and Colloid Science*; Matijevic, E., Ed.; Plenum Press: New York, 1993; Vol. 15, p 1. (b) Riess, G.; Hurtrez, G.; Bahadur, P. In *Encyclopedia of Polymer Science and Engineering*, 2nd ed.; Mark, H. F., Bikales, N. M., Overberger, C. G., Menges, G., Eds.; Wiley: New York, 1985; Vol. 2, pp 324–436.
- (5) See Procházka, K.; Martin, T. J.; Munk, P.; Webber, S. E. *Macromolecules*, following paper in this issue.
- (6) Allen, R. D.; Long, T. E.; McGrath, J. *Polym. Bull.* **1986**, *15*, 127.
- (7) Nugay, N.; Küçükyau, Z. *Eur. Polym. J.* **1995**, *31*, 1983.
- (8) Procházka, K.; Glöckner, G.; Hoff, M.; Tuzar, Z. *Makromol. Chem.* **1979**, *185*, 1187.
- (9) *Polymer Handbook*; Brandrup, J.; Immergut, E. H., Eds.; Wiley-Interscience: New York, 1989.
- (10) See, for example: Berne, B. J.; Pecora, R. *Dynamic Light Scattering: with applications to chemistry, biology, and physics*; Wiley-Interscience: New York, 1976.
- (11) (a) Misra, S.; Mattice, W. L.; Napper, D. H. *Macromolecules* **1994**, *27*, 7090. (b) Zhulina, E. B.; Birshtein, T. M.; Borisov, O. V. *Macromolecules* **1995**, *28*, 1491. (c) Israëls, R.; Leermakers, F. A. M.; Fleer, G. J.; Zhulina, E. B. *Macromolecules* **1994**, *27*, 3249. (d) Lyatskaya, Yu. V.; Leermakers, F. A. M.; Fleer, G. J.; Zhulina, E. B.; Birshtein, T. M. *Macromolecules* **1995**, *28*, 3562.
- (12) Berlman, I. B. *Energy Transfer Parameters of Aromatic Compounds*; Academic Press: New York, 1973.
- (13) Berlman, I. B. *Handbook of Fluorescence Spectra of Aromatic Molecules*; Academic Press: New York, 1971.
- (14) Dong, D. C.; Winnik, F. A. *Photochem. Photobiol.* **1982**, *35*, 17.
- (15) (a) Zhao, C.-L.; Winnik, M. A.; Reiss, G.; Croucher, M. D. *Langmuir* **1990**, *6*, 514. (b) Wilhelm, M.; Zhao, C.-L.; Wang, Y.; Xu, R.; Winnik, M. A. *Macromolecules* **1991**, *24*, 1033. (c) Nakashima, K.; Winnik, M. A.; Dai, K. H.; Kramer, E. J.; Washiyama, J. *Macromolecules* **1992**, *25*, 6866.
- (16) Acree, W. E.; Tucker, S. A.; Wilkins, D. C. *J. Phys. Chem.* **1993**, *97*, 11199.
- (17) (a) Arca, E.; Tian, M.; Webber, S. E.; Munk, P. *Int. J. Polym. Anal. Characterization* **1995**, *2*, 31. (b) M. Morrison *et al.*, work in progress.
- (18) Yalkowsky, S. H.; Banerjee, S. *Aqueous Solubility*; Marcel Dekker, Inc: New York, 1992.

MA960630E